



Reaction rate uncertainty quantification and  
propagation, variance-covariance



- Single irradiation pulse followed by cooling
- Multiple irradiation pulses
  - changing flux amplitude
  - cooling
- Multi-step
  - changing flux amplitude and spectrum
  - changing cross-section (e.g., temperature dependence)
  - cooling
- Pathways and sensitivity for all cases



- Extracts and reduces nuclear and radiological data
- Solves rate equations for time evolution of inventory
- Computes and outputs derived radiological quantities
- Identifies and quantifies key reactions and decay processes:
  - dominant nuclides
  - pathways and uncertainty
  - Monte-Carlo sensitivity and uncertainty
  - reduced model calculations
- Uncertainty calculation
  - input cross-section and decay uncertainties
  - output uncertainties for all radiological quantities

- Condense run extracts from decay files:
  - decay constant  $\lambda$
  - decay constant uncertainty  $\Delta\lambda$
- Collapse constructs flux spectrum weighted averages:

➤ Library input

- cross-section vs energy
- covariances vs energy
- flux spectrum vs energy

$$W_i = \frac{\phi_i}{\sum_{i=1}^N \Phi_i}$$

$$\overline{XS} = \sum_{i=1}^n W_i X_i$$



Data used in code

- collapsed cross-section
- collapsed uncertainty  $\Delta$

$$\overline{XS}$$

- reactions X and Y
- energy bins i and j  $\in [1, N]$  with  $N = 709$
- uses  $\text{Cov}(X_i, Y_j)$  for  $X \neq Y$  only in Monte-Carlo
- collapse  $\text{Cov}(X_i, X_j)$  to get uncertainty  $\Delta$  for  $\bar{X}$

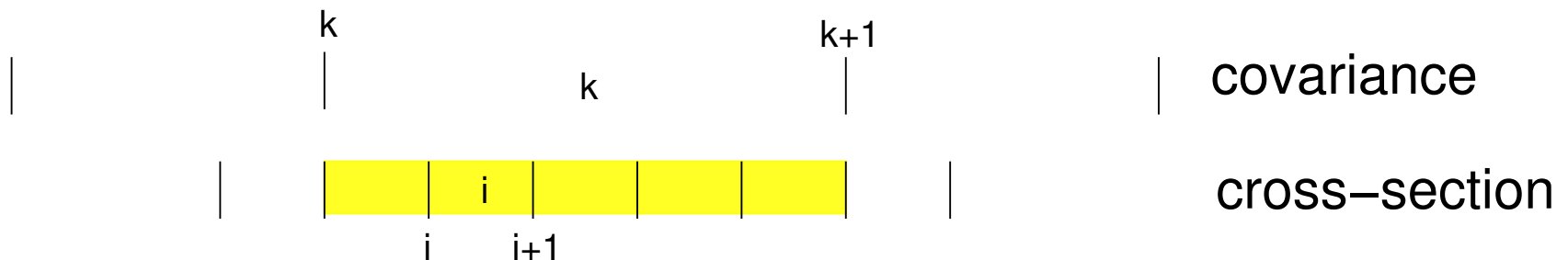
1 TENDL, 3 EAF

$$var = \sum_{i=1}^N \sum_{j=1}^N W_i W_j \text{Cov}(X_i, X_j); \quad \Delta = \{1|3\} \sqrt{var} / \bar{X}$$

- Collapse  $\text{Cov}(X_i, Y_j)$  to get  $\text{Cov}(\bar{X}, \bar{Y})$  for  $X \neq Y$
- Cov data in ENDF file 33 & 40, NI type LB=1, 5, 6
- Cov data in wider energy bins k  $\in [1, M]$ ,  $M \sim 40$

The projection operator  $S_i^k$  maps cross-section energy bins to covariance energy bins

$$S_i^k = \begin{cases} 1 & \text{bin } i \text{ in bin } k \\ 0 & \text{otherwise} \end{cases}$$



The ENDF style covariance data forms, different LB' s are read directly without the need of pre-processing

Using  $S_i^k$ , the formula to construct estimates of the covariance matrix are as follows:

$$LB = 1 : \quad Cov(X_i, X_j) = \sum_{k=1}^M S_i^k S_j^k F_k X_i X_j$$

→→  $LB = 5 : \quad Cov(X_i, Y_j) = \sum_{k=1}^M \sum_{k'=1}^M S_i^k S_j^{k'} F_{kk'} X_i Y_j$

→→  $LB = 6 : \quad Cov(X_i, Y_j) = \sum_{k=1}^M \sum_{k'=1}^{M'} S_i^k S_j^{k'} F_{kk'} X_i Y_j$

$$LB = 8 : \quad Cov(X_i, X_j) = \sum_{k=1}^M S_i^k S_j^k 1000 F_k \quad (Koning)$$

$$(or = \sum_{k=1}^M S_i^k \delta_{ij} 1000 F_k)$$

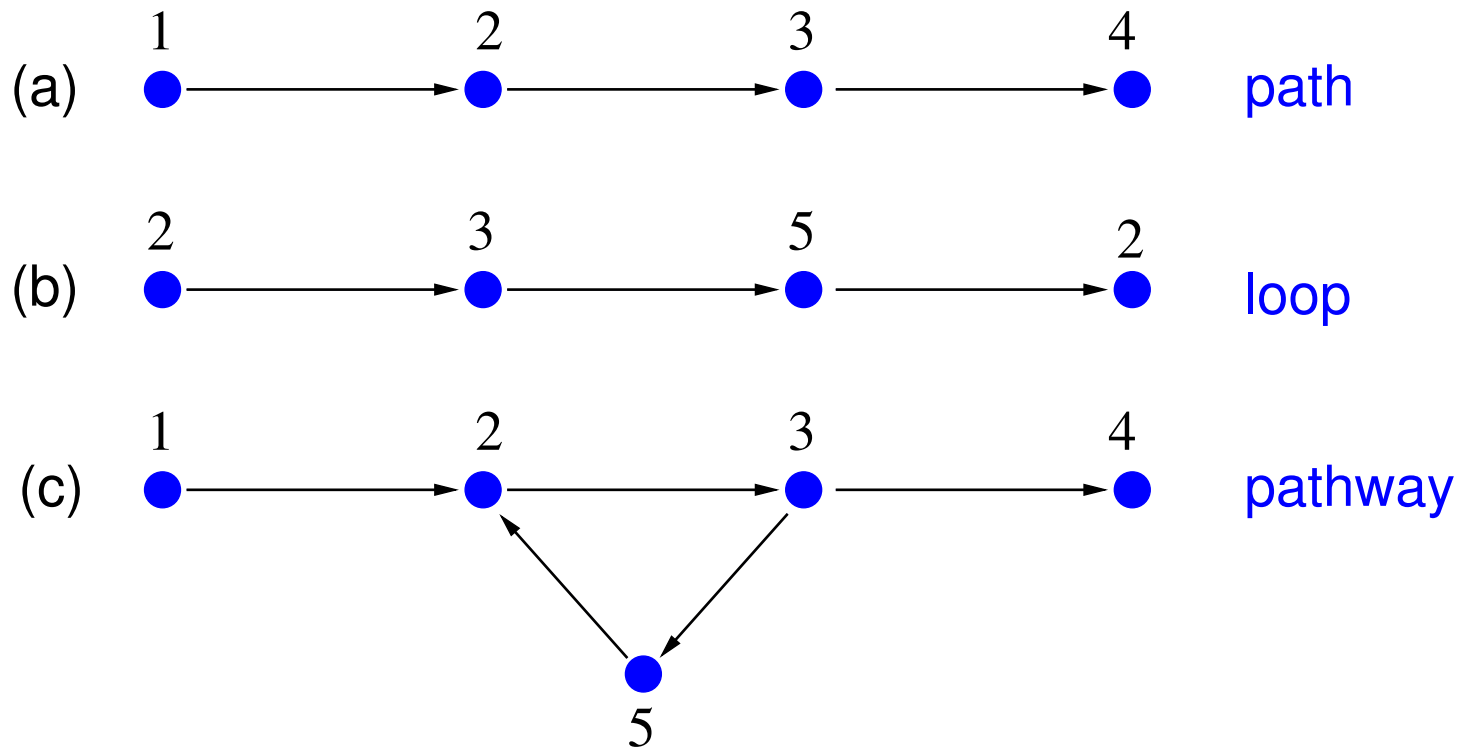
The LB=1 case is the one that was applied to the computation of  $\Delta$  for the EAF's libraries

- Given  $\{\overline{XS}, \lambda\}$ 
  - select irradiation scenario
  - solve for radiological quantities
- Use  $\{\Delta X, \Delta \lambda\}$  to estimate uncertainties
  - method 1: pathways to dominant nuclides
  - method 2: Monte-Carlo sensitivity
  - method 3: reduced model Monte-Carlo sensitivity



- Pathways are used to identify the dominant contributors to the activation products for the specific irradiation scenario under consideration.
- This makes the calculation of uncertainties more practicable for all methods (random-walk approximation and Monte-Carlo).
- The standard uncertainty output uses a random-walk approximation to estimate error bounds.
- This estimate is much quicker than Monte-Carlo, but is likely to give larger bounds since it ignores many possible correlations.

- given initial inventory and irradiation scenario
- sort dominant nuclides at end of irradiation phase
  - `topxx` (=20) controls number
  - 8 categories - activity, heat production, dose, etc.
- construct pathways from initial to dominant nuclides
  - `path_floor` (=0.005) and `loop_floor` (=0.01)
  - iterate on single-visit breadth-first search tree
- compute inventory contributions of pathways
- construct error estimate



- keep pathways providing  $> \text{path\_floor}$  of target inventory
- keep loop providing  $> \text{loop\_floor}$  of pathway inventory

$$Q = \sum_{t \in S_t} q_t; \quad (\Delta Q)^2 = \sum_{t \in S_t} \left( \frac{\Delta N_t}{N_t} \right)^2 q_t^2$$

$$(\Delta N_t)^2 = \sum_{p \in S_o} \Delta_{tp}^2 N_{tp}^2 + \sum_{a \in S_{sa}} \left( \sum_{p \in S_a} |\Delta_{tp}| N_{tp} \right)^2$$

$$\Delta_{tp}^2 = \sum_{e \in S_e} \sum_{r \in S_r} \left[ \frac{R_r \Delta_r}{R_e} \right]^2 + \sum_{e \in D_e} \left[ \frac{\Delta \lambda_e}{\lambda_e} \right]^2$$

- $N_t$  (atoms) and  $q_t$  (radiological quantity) from rate equation
- $\Delta_{tp}$ ,  $N_{tp}$ ,  $\Delta N_t$  from pathways
- $R_r$  and  $R_e$  pulse averaged reaction rates
- reactions uncorrelated, fission correlated



## UNCERTAINTY ESTIMATES (cross sections only)

Uncertainty estimates are based on pathway analysis for the irradiation phase

Total Activity is 1.25070E+14 +/- 8.52E+11 Bq. Error is 6.81E-01 % of the total.  
Total Heat Production is 3.60059E-02 +/- 3.09E-04 kW. Error is 8.60E-01 % of the total.  
Total Gamma Dose Rate is 5.63098E+04 +/- 5.04E+02 Sv/hr. Error is 8.95E-01 % of the total.  
Total Ingestion Dose is 1.38528E+05 +/- 1.17E+03 Sv. Error is 8.45E-01 % of the total.  
...

Target nuclide Sc 44 99.557% of inventory given by 8 paths

path 1 20.048% Ti 46 ---(R)--- Sc 45 ---(R)--- Sc 44 ---(S)---  
98.16%(n,np) 100.00%(n,2n)  
1.84%(n,d)

path 2 12.567% Ti 46 ---(R)--- Sc 45 ---(R)--- Sc 44m---(b)--- Sc 44 ---(S)---  
98.16%(n,np) 100.00%(n,2n) 100.00%(IT)  
1.84%(n,d) 0.00%(n,n)

path 3 11.143% Ti 46 ---(R)--- Sc 45m---(d)--- Sc 45 ---(R)--- Sc 44 ---(S)---  
96.62%(n,np) 100.00%(IT) 100.00%(n,2n)  
3.38%(n,d)

...

- The TENDL library contains MF=33, LB=6 data for different reactions  $X_1, X_2, \dots$  for a given parent, i.e.,  $p(n, X_1)d_1, p(n, X_2)d_2, \dots$
- These covariance data  $\text{cov}(X_1, X_2)$  for  $X_1, X_2$  are stored as fractional values  $f^{X_1 X_2}$  and are tabulated in the same energy bins as used respectively for the LB=5 covariance data  $f^{X_1 X_1}, f^{X_2 X_2}$  for reactions  $X_1, X_2$
- If the COVARIANCE keyword is used, FISPACT-II reads these data for all energy bins  $k$  and  $l$  and corrects for any instances where

$$\left| \frac{f_{kl}^{X_1 X_2}}{\sqrt{f_{kk}^{X_1 X_1} f_{ll}^{X_2 X_2}}} \right| > 1$$

- Then the code uses the corrected data to compute collapsed covariance  $\text{cov}(X_1, X_2)$ . Covariances are mapped to MF=10 by assuming that all isomeric daughters of a given pair of reactions with rates  $X_1$ ,  $X_2$  have the same collapsed correlation function,  $\text{corr}(X_1, X_2)$ .
- Tables of all reactions which have covariance data and their collapsed covariances and correlations are printed by the collapse run. Inspection of these data will show those cases where the assumption of zero correlation between reactions of a given parent is not good.
- The effect of non-negligible correlations on uncertainties may be introduced into Monte-Carlo sensitivity calculations by choosing distributions of sample cross-sections to have the same variances and covariances as given by the TENDL data.

- reference run + S inventory calculations
- independent  $\{X_i^s; i = 1, \dots, I; s = 1, \dots, S\}$
- dependent  $\{Y_j^s; j = 1, \dots, J; s = 1, \dots, S\}$
- independent variables selected using random numbers
  - normal, log-normal, uniform, log-uniform
  - means  $\langle X_i \rangle$  and standard deviations  $\langle \Delta X_i \rangle$
- compute summary results:
  - means
  - standard deviations
  - Pearson correlation coefficients
- output full data for post-processing



- output mean and standard deviation

$$\bar{X}_i = \frac{1}{S} \sum_{s=1}^S X_i^s \quad \Delta X_i = \sqrt{\frac{1}{S-1} \sum_{s=1}^S [(X_i^s)^2 - \bar{X}_i^2]}$$
$$\bar{Y}_j = \frac{1}{S} \sum_{s=1}^S Y_j^s \quad \Delta Y_j = \sqrt{\frac{1}{S-1} \sum_{s=1}^S [(Y_j^s)^2 - \bar{Y}_j^2]}$$

- Pearson correlation coefficient

$$r_{ij} = \frac{\sum_s X_i^s Y_j^s - S \bar{X}_i \bar{Y}_j}{\Delta X_i \Delta Y_j}$$

- controlled by keywords SENSITIVITY, MCSAMPLE, MCSEED, COVARIANCE



## Base cross section data

index				parent				daughter				sigma	sigma_unc
i	zai	nuc_no	name	i	zai	nuc_no	name	i	zai	nuc_no	name	cm**2	
1	220460	233	Ti 46	1	210460	219	Sc 46	1	210460	219	Sc 46	0.39039E-25	0.35942E-01
2	220460	233	Ti 46	2	210461	220	Sc 46m	2	210461	220	Sc 46m	0.10142E-25	0.35942E-01
3	220480	235	Ti 48	3	210480	222	Sc 48	3	210480	222	Sc 48	0.11049E-25	0.87272E-02

...

## Output nuclides

j	zai	nuc_no	name
1	210460	219	Sc 46
2	210470	221	Sc 47
3	210480	222	Sc 48

...

Normal, x cutoff = [ -3.0000 , 3.0000 ] std dev ← Normal random sampling

j	atoms_base	atoms_mean	atoms_unc
1	2.50290E+20	2.49955E+20	2.46164E-02
2	7.99801E+18	7.99665E+18	1.68690E-03
3	9.91006E+18	9.90588E+18	8.55649E-03

...

## Correlation coefficients

j\i	1	2	3	4
1	9.66468E-01	- - - -	- - - -	- - - -
2	- - - -	- - - -	- - - -	9.99810E-01
3	- - - -	- - - -	1.00000E+00	- - - -
4	- - - -	- - - -	9.99993E-01	- - - -
5	- - - -	- - - -	- - - -	-9.99911E-01
6	- - - -	- - - -	-9.60898E-01	- - - -
7	-9.66478E-01	- - - -	- - - -	- - - -

← reactions

↑ output nuclides



- UKDD-2012 decay - 3873 nuclides
- calculation includes all nuclides in master index
- INDEXPATH generates reduced master index from pathways
  - typically few 10s of nuclides
  - number adjustable by pathway parameters
- reduced master index run vs full run to validate discards
- Monte-Carlo sensitivity for reduced master index runs
  - faster + comparable answers



## Self shielding of resonant channels

- Probability tables, sub-group method
  - High fidelity resonances

CALENDF probability tables are used to model dilution effects in the computation of the effective cross-sections

cal-mt	description	mt in set
2	elastic scattering	2
101	absorption (no outgoing neutron)	102 103 107
18	fission total	18
4	inelastic scattering (emitting one neutron)	4 11
15	multiple neutron production (excluding fission)	5 16 17 37

$$\sigma_{\text{eff}}(x, n) = \sigma_{\text{eff}}(g, x, n) \text{ and } p(x, n) = p(g, x, n)$$

where

g = energy group number

x = macro-partial (or total) index

n = quadrature index

# Cross section, PT distribution, discretization

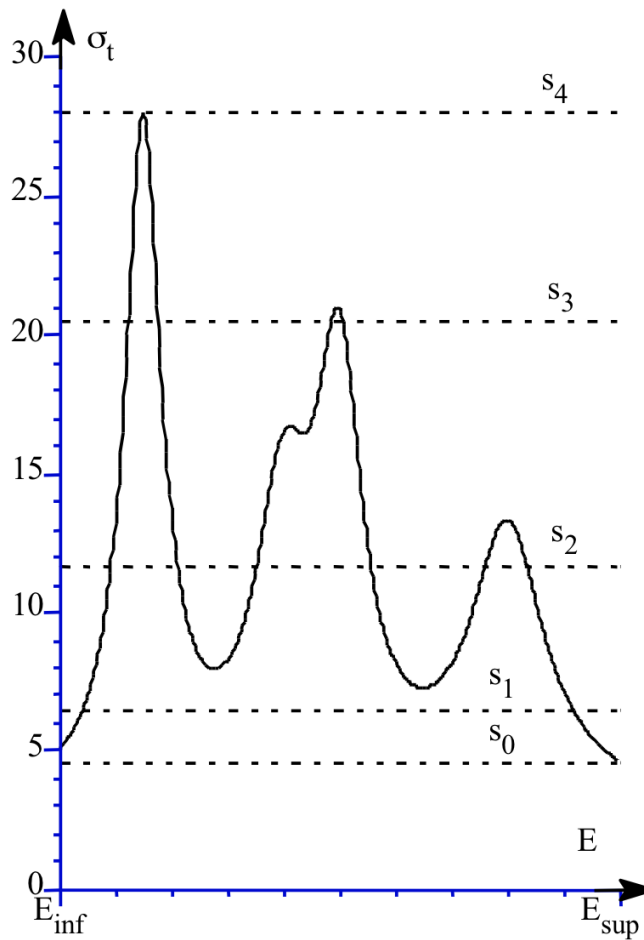
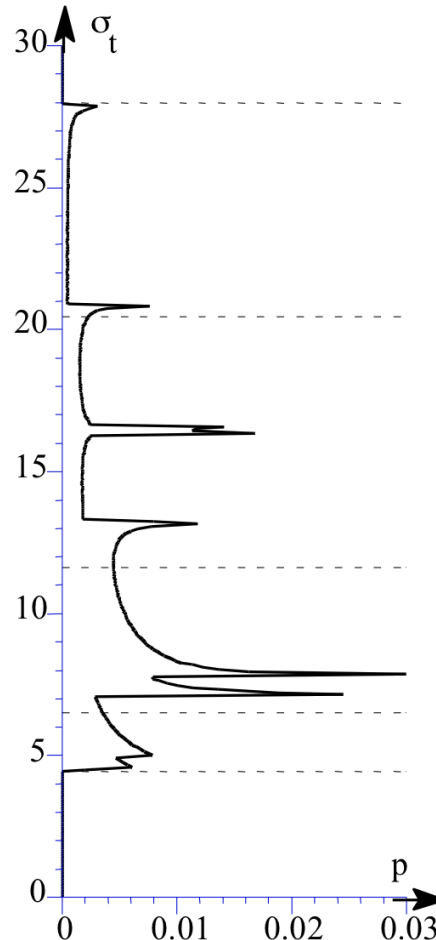
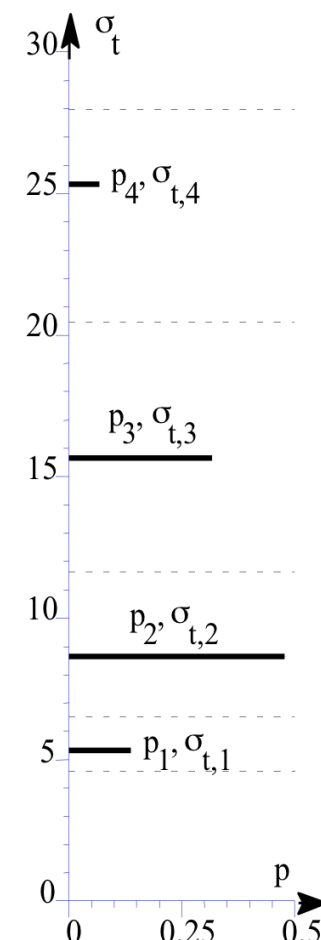


**Fig. 1a** Cross section versus energy



**1b** Exact PT distribution



**1c** PT discretisation

$$\frac{1}{G} \int_{E_{\text{inf}}}^{E_{\text{sup}}} \sigma_t^n(E) dE = \int_{\sigma_{\text{min}}}^{\sigma_{\text{max}}} p(\sigma_t) \sigma_t^n d\sigma_t = \sum_{i=1}^{i=N} p_i \sigma_{t,i}^n$$

# Padé approximant and Gauss Quadrature

The moments having been computed, the probability table is established:

$$\begin{aligned} I(z) &= \int \frac{p(x)}{1-zx} dx = \underbrace{M_0 + M_1 z + M_2 z^2 + \dots + M_{2N-1} z^{2N-1}}_{2N \text{ moments}} + R_{2N} z^{2N} \\ &= \frac{b_0 + b_1 z + b_2 z^2 + \dots + b_{N-1} z^{N-1}}{\underbrace{1 + a_1 z + a_2 z^2 + \dots + a_N z^N}_{Q_{N,N-1} = \text{PADE approximant}}} + R'_{2N} z^{2N} \\ &= \frac{b_0 + b_1 z + \dots + b_{N-1} z^{N-1}}{\prod_{i=1}^N (1 - zx_i)} + R'_{2N} z^{2N} = \sum_i \underbrace{\frac{p_i}{1 - zx_i}}_{p_i, x_i = \text{quad. table}} + R'_{2N} z^{2N} \end{aligned}$$

The second line is the Padé approximant that introduces an approximate description of higher moment order

The effective cross section can be calculated from either the pointwise cross section or the probability table as follows:

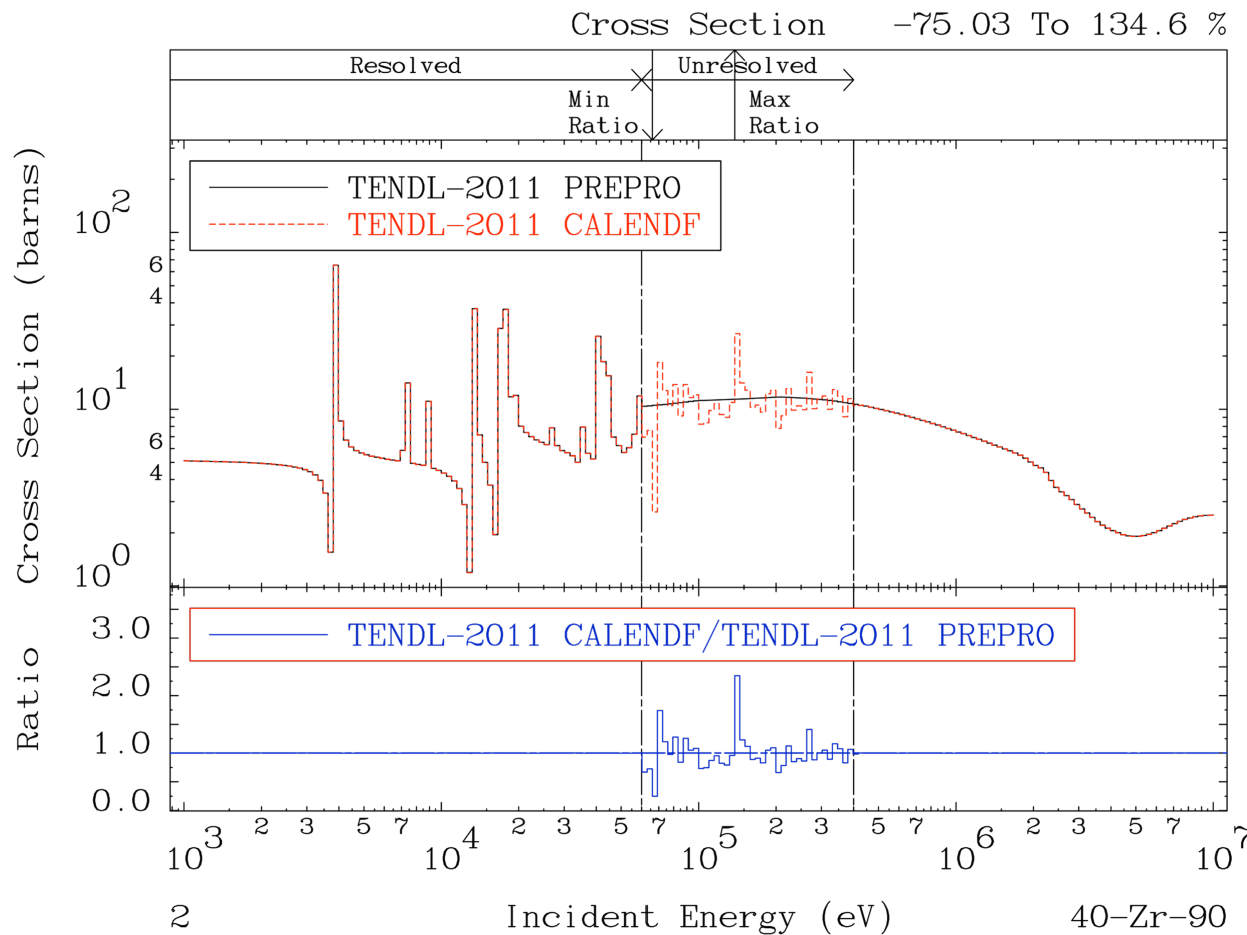
$$\sigma_{x,eff,quad.}(\sigma_d) = \frac{\sum_{i=1}^{i=N} \frac{p_i \sigma_{x,i}}{\sigma_{t,i} + \sigma_d}}{\sum_{i=1}^{i=N} \frac{p_i}{\sigma_{t,i} + \sigma_d}}$$

When the dilution is infinite this formula becomes:

$$\sigma_{x,eff,quad.} = \sum_{i=1}^{i=N} p_i \sigma_{x,i}$$



# Effective cross sections comparison



From 0.1 eV to the end  
of the URR

Uniquely accessible  
SSF's in the URR !!

Self Shielding Factor

The probability tables from CALENDF are used in conjunction with fine 709 or 1102 group data. They are given at 3 temperatures: 293.6, 600 and 900 Kelvin

The dilution  $d(p; g)$  for a given nuclide  $p$  and energy group  $g$  is computed using a weighted sum over all the nuclides,  $q = 1; Q$  in the mixture. The first approximation for the fraction  $f_q$  uses the total cross-sections :

$$d^{(0)}(p, g) = \sum_{\substack{q=1 \\ p \neq q}}^Q \frac{f_q \sigma^{LIB-tot}(q, g)}{f_p}$$

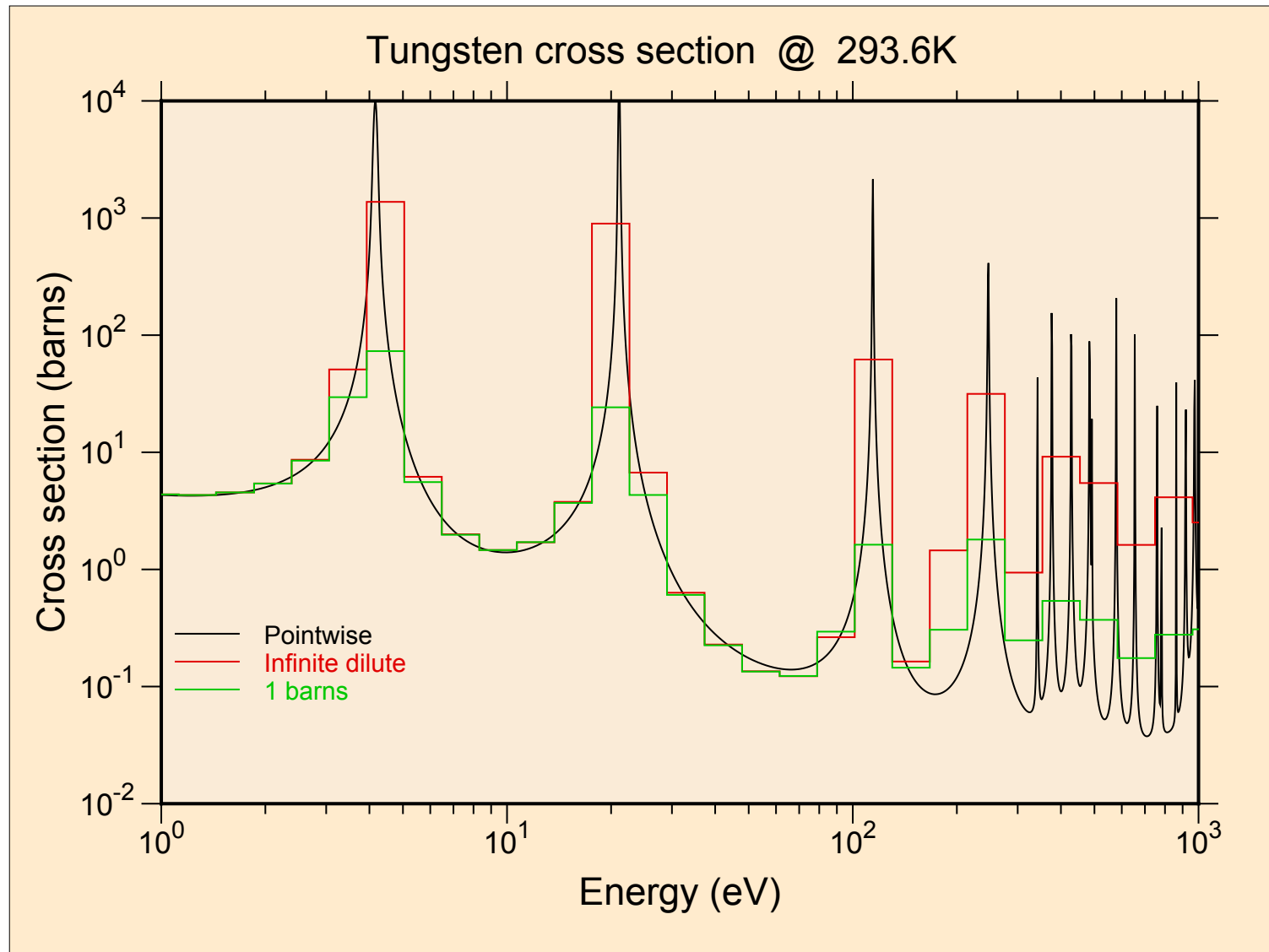
where

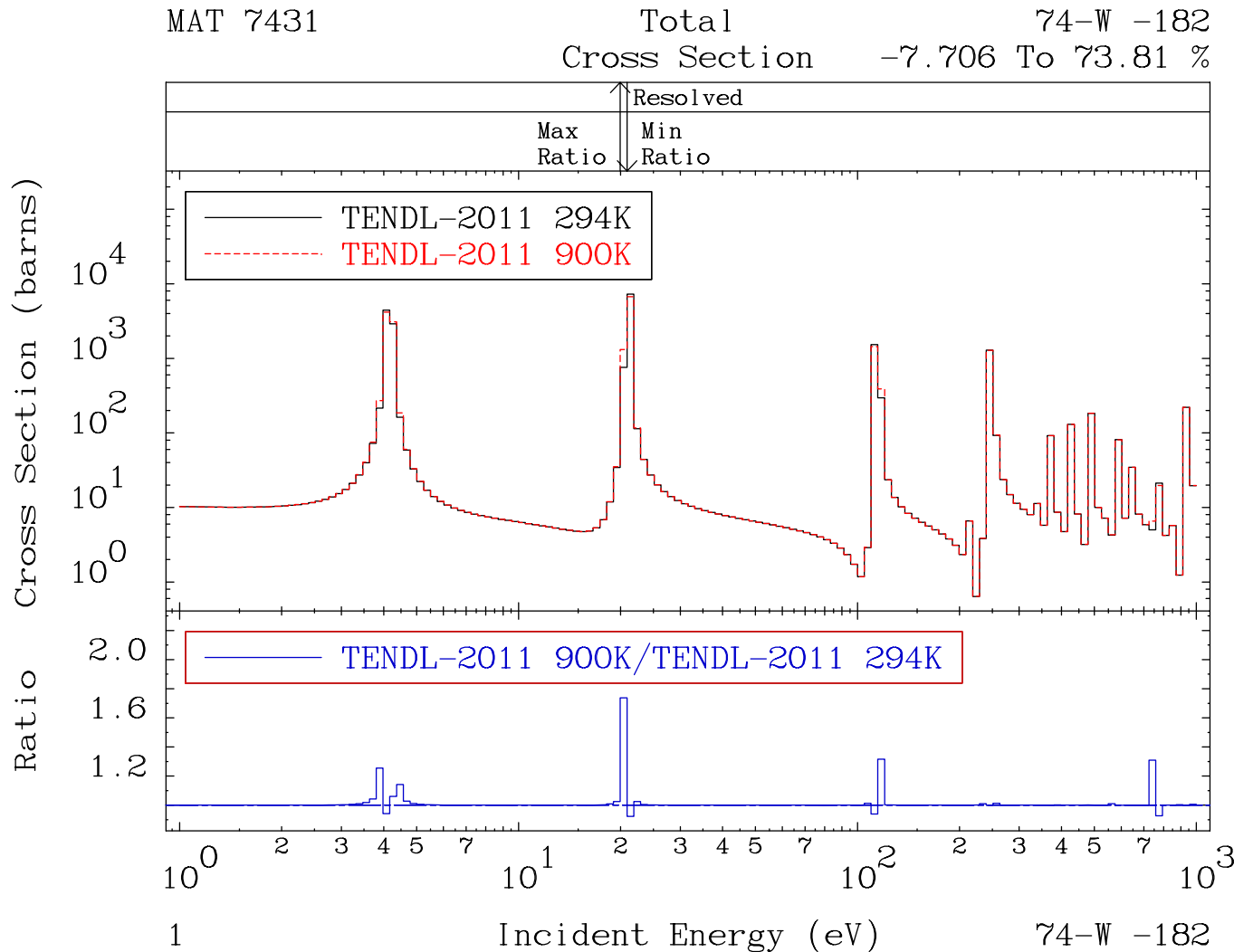
$$\sigma^{LIB-tot}(p, g) = \sum_{y=1}^Y \sigma^{LIB}(p, g, y)$$

Over the energy range for which the probability table data are available, the above approximation is iteratively refined using:

$$S^{(i)}(g) = \sum_{q=1}^Q f_q \sigma^{LIB-tot}(q, g) \left( \frac{\sigma^{tot}(q, g, d^{(i)}(q, g))}{\sigma^{tot}(q, g, \infty)} \right)$$
$$d^{(i+1)}(p, g) = \frac{S^{(i)}(g)}{f_p} - \sigma^{LIB-tot}(p, g) \left( \frac{\sigma^{tot}(p, g, d^{(i)}(p, g))}{\sigma^{tot}(p, g, \infty)} \right)$$

# Effective cross section: dilution effects





Giant resonances  
dominate the  
reaction rate

The effect is not negligible around the resonances



## Self shielding of resonant channels

- thin and thick target yields
- High fidelity resonance

- thin and thick target yields
- accounts approximately for target geometry
- applicable to thick targets
- handles foils, wires, spheres and finite cylinders
- uses one physical length scale to represent the target: the “effective length”  $y$

Type ID	Geometry	Dimension(s)	$Y$
1	foil	thickness ( $t$ )	$y=1.5t$
2	wire	radius ( $r$ )	$y=2r$
3	sphere	radius ( $r$ )	$y=r$
4	cylinder	radius ( $r$ ), height ( $h$ )	$y=1.65rh(r+h)$

- theory of radioisotope production
- production rates and cross-sections
- saturation factors and practical yields
- model uses resonance parameters from the Resolved Resonance Range
- model includes the effects of neutron loss through radiative capture
- model includes effects of neutron energy diffusion through elastic scattering

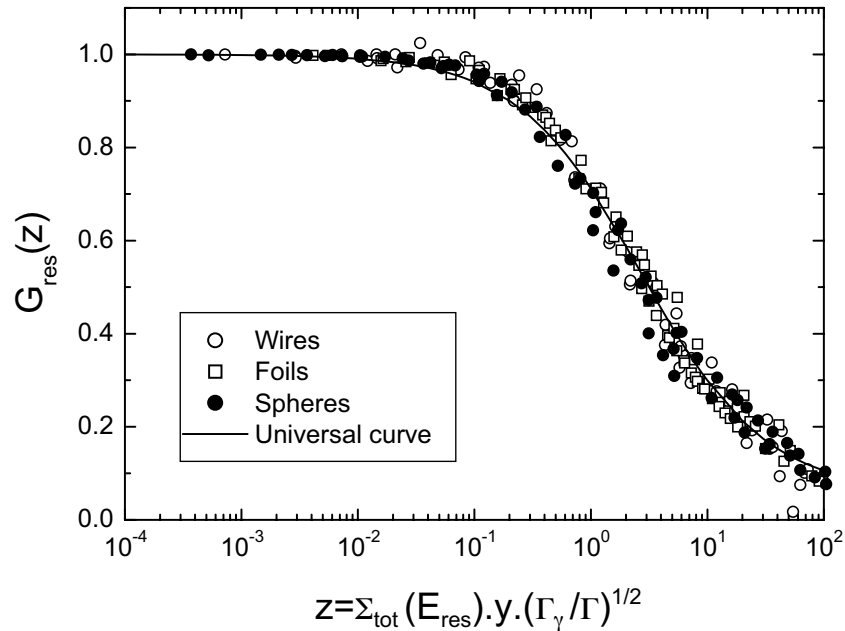
- one resonance in a pure target
- dimensionless parameter to combine the physical effective length with the nuclear parameters

$$z = \Sigma_{tot}(E_{res}) y \sqrt{\frac{\Gamma_{\gamma}}{\Gamma}}$$

- where
  - $\Sigma_{tot}(E_{res})$  is the macroscopic cross-section at the energy  $E_{res}$  of the resonance peak
  - $\Gamma_{\gamma}$  is the radiative capture width
  - $\Gamma$  is the total resonance width
  - $y$  “effective length”
- Self-shielding factor  $G_{res}$  is defined in terms of  $z$  only

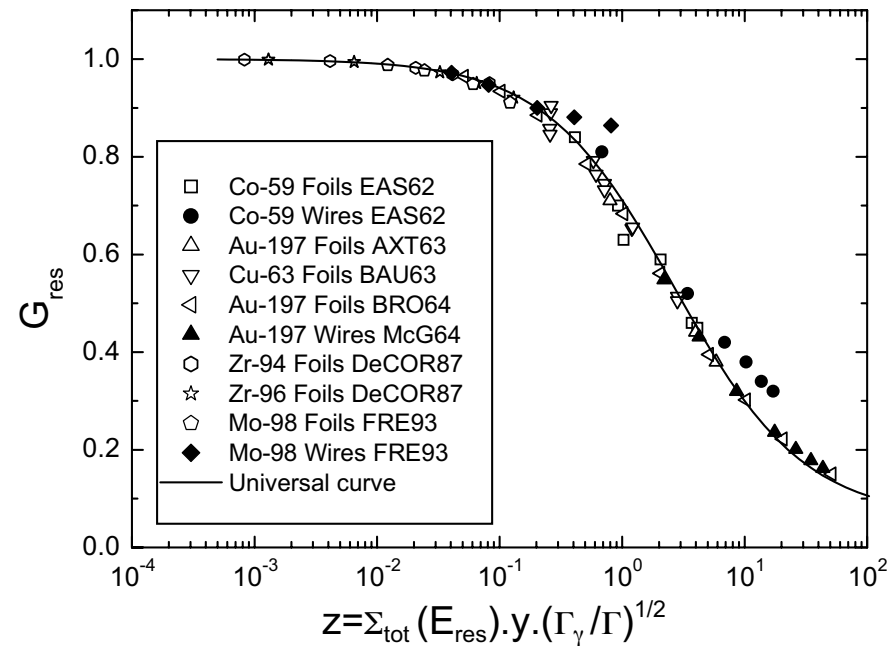


Baumann, 1963; Yamamoto and Yamamoto, 1965; Lopes, 1991



Target geometry

Experimental self shielding factor



$$G_{res}(z) = \frac{A_1 - A_2}{1 + \left(\frac{z}{z_0}\right)^p} + A_2$$

- this is the “universal sigmoid curve” for the model
- the parameters have been determined empirically to be a good fit to experimental data
- preferred values are:
  - $A_1 = 1.000 \pm 0.005$
  - $A_2 = 0.060 \pm 0.011$
  - $Z_0 = 2.70 \pm 0.09$
  - $p = 0.82 \pm 0.02$

- extend model to a group of separated resonances
- still considering a pure target: one nuclide
- assign a weight to each resonance

$$w_i = \left( \frac{\Gamma_\gamma}{E_{res}^2} \cdot \frac{g\Gamma_n}{\Gamma} \right)_i$$

where

- $\Gamma_n$  is the neutron scattering width
- $g$  is the statistical factor,  $(2J + 1)/(2(2I + 1))$
- $J$  is the spin of the resonance state
- $I$  is the spin of the target nucleus
- form an average self-shielding factor from all resonances of interest

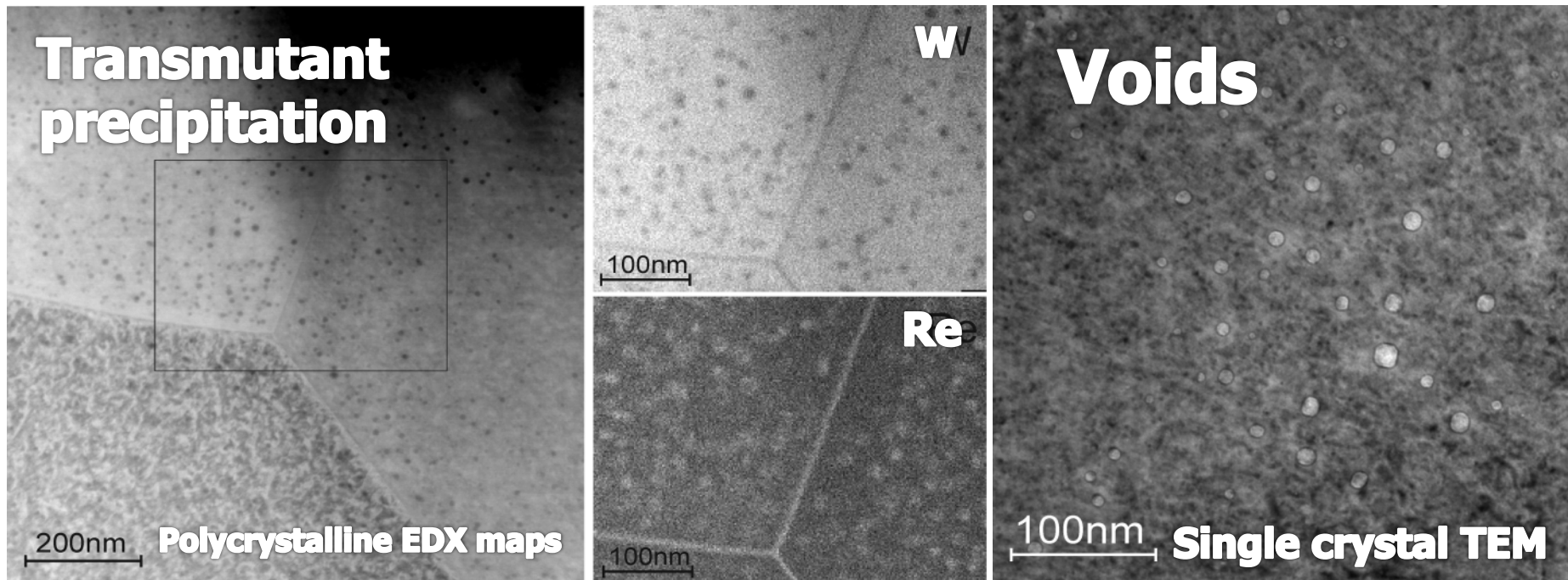
$$\langle G_{res} \rangle = \frac{\sum w_i G_{res}(z_i)}{\sum w_i}$$

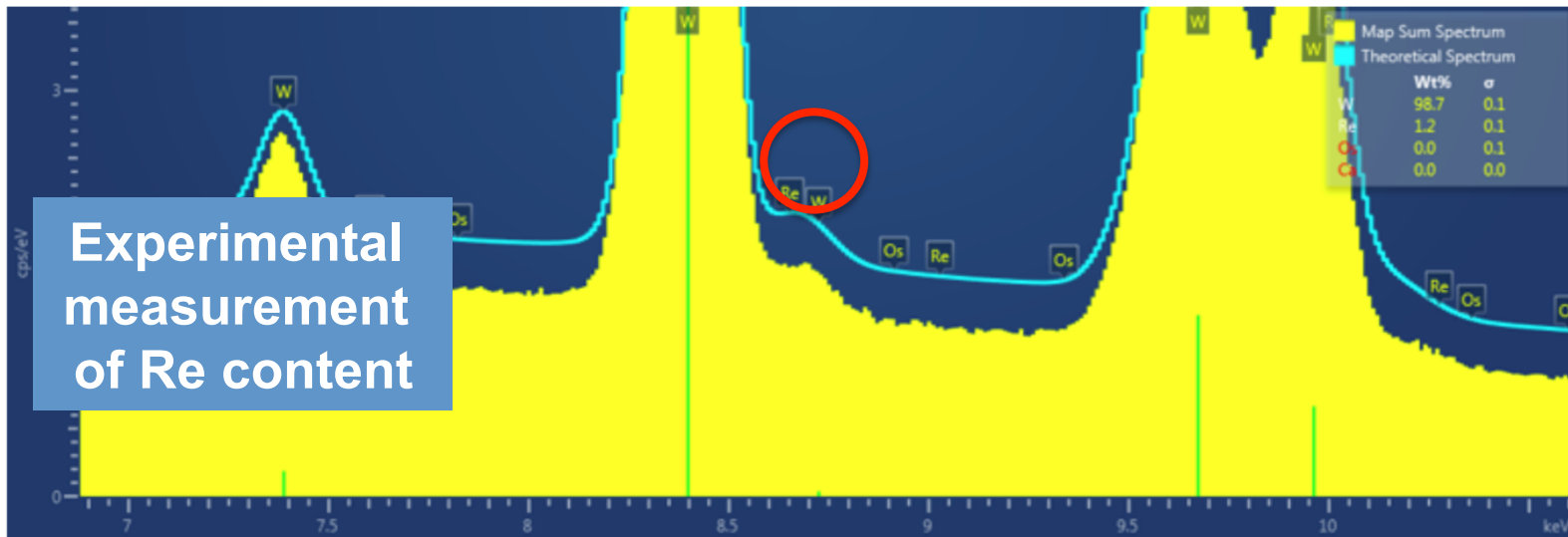
- extend  $\langle G_{\text{res}} \rangle$  to form the average for resonances of a mixture of nuclides
- assume the resonances of different nuclides do not overlap significantly
- make  $\langle G_{\text{res}} \rangle$  energy dependent by taking averages separately for each energy bin used for the group-wise cross-sections
- use Fröhner's simple expression for the peak cross-section of each resonance (not available from the GENDF data)

- universal curve model provides an alternative to probability table self shielding
- use  $\langle G_{\text{res}} \rangle(E)$  to scale down energy-dependent cross-sections before cross-section collapse
- $\langle G_{\text{res}} \rangle(E)$  reduces the neutron flux, so apply it to all cross-sections
- target geometry specified with  
**SSFGEOMETRY** type length<sub>1</sub> <length<sub>2</sub> >
- use resonances from mixture specified with **SSFFUEL** or **SSFMASS**
- PRINTLIB 6 now generates a table of all cross-sections with  $\langle G_{\text{res}} \rangle$  reduction factors

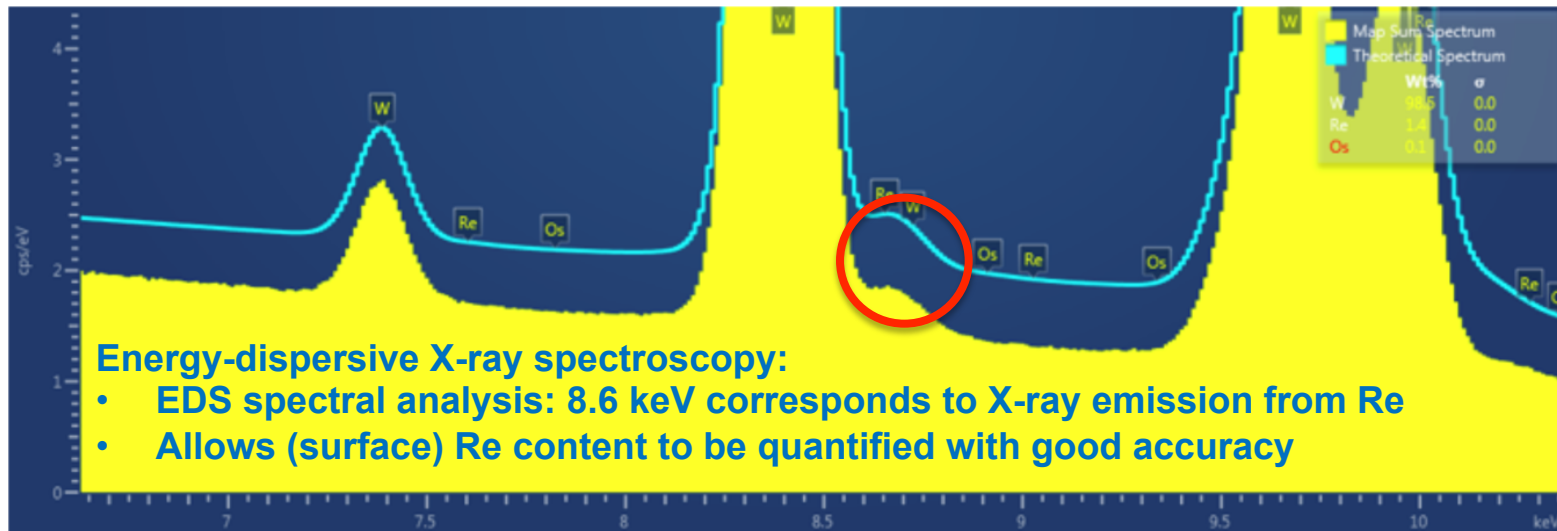
## Neutron-irradiated tungsten: comparison between experiment and simulation

- W irradiated in the high-flux reactor (HFR) @ NRG, Petten
- Has been cooling for a number of years (see later)
- Only now is it starting to be analyzed
- Full of defects & voids, and some percentage of transmutation products – mostly rhenium





Petten Single Crystal (1.2wt% Re measured)



Petten Polycrystalline (1.4wt% Re measured)

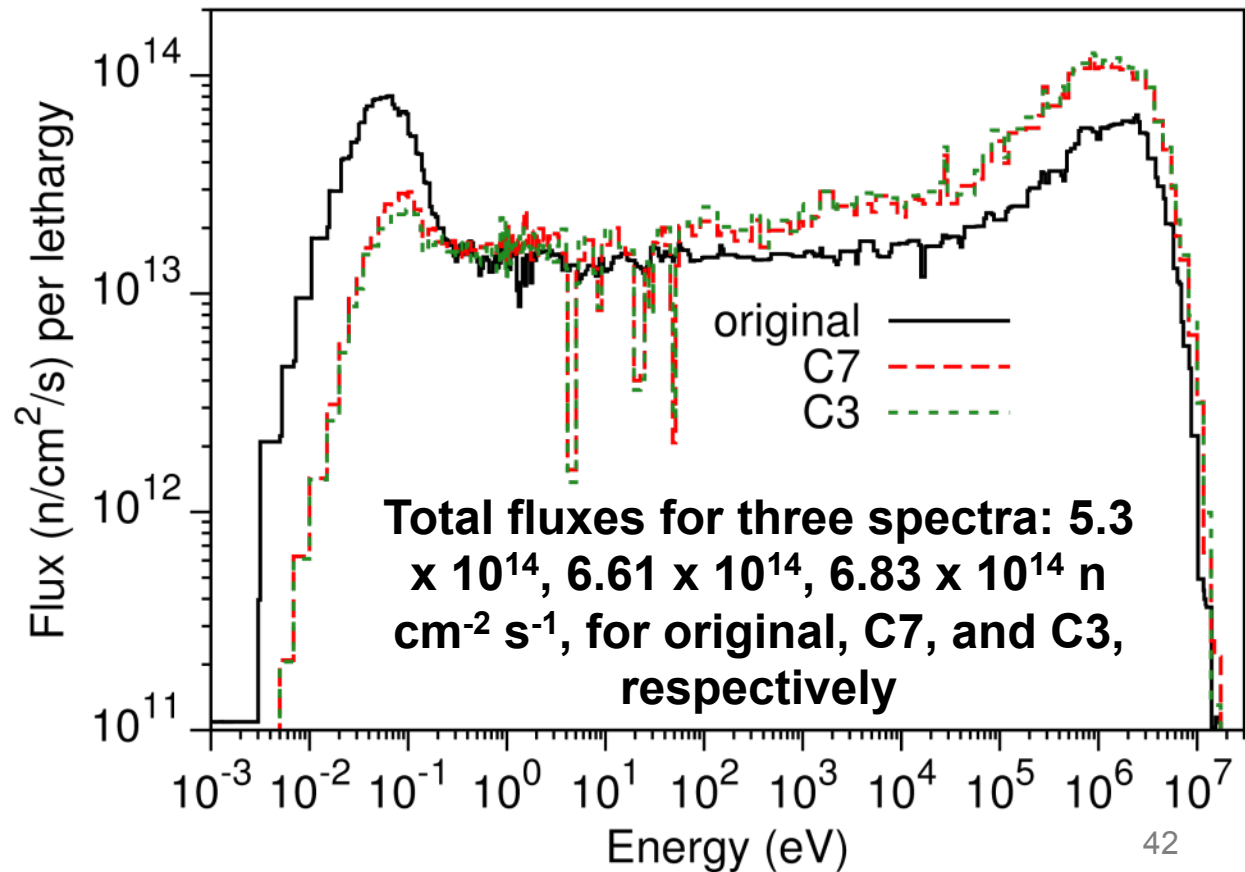


- W irradiated under EXTREMAT-II in 2008 & 2009
- Target of 282 days of irradiation (10 cycles), but in fact only irradiated in 8 cycles & in two different positions:

Position	Cycle	EFPD	Start date	End date
C7	08-May	30.72	22-May-08	22-Jun-08
	08-Jun	29.71	28-Jun-08	28-Jul-08
C3	09-Jan	27.69	12-Feb-09	12-Mar-09
	09-Feb	24.99	01-Apr-09	26-Apr-09
	09-Mar	30.77	29-Apr-09	30-May-09
	09-Apr	24.71	02-Jun-09	27-Jun-09
	09-May	17.61	30-Jun-09	18-Jul-09
	09-Jun	22.06	17-Aug-09	08-Sep-09
<b>Total</b>		<b>208.26</b>		

- EFPD – effective full power days

- Samples were positioned next to another experiment with very strong thermal neutron absorption properties
  - W exposed to a lower than normal (for HFR) fraction of thermal neutrons creating reduced transmutation
- **New spectra calculated for the approximate axial position of EXTREMAT-II, averaged over radial extent of experiment and over around 4 cm of height**



- To correctly account for self-shielding in all isotopes of W
  - During collapse:

```
PROBTABLE 1 1
SSFCHOOSE 1 0 W
SSFMASS 1.0 1
W 100.0
GETXS 1 709
```

- Other option (`SSFFUEL`) allows explicit specifications of isotopes to self-shield

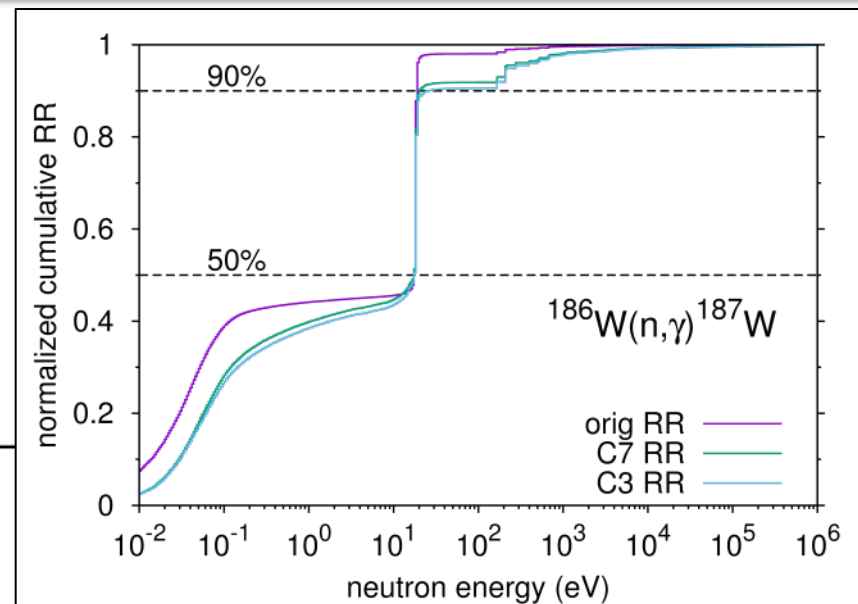
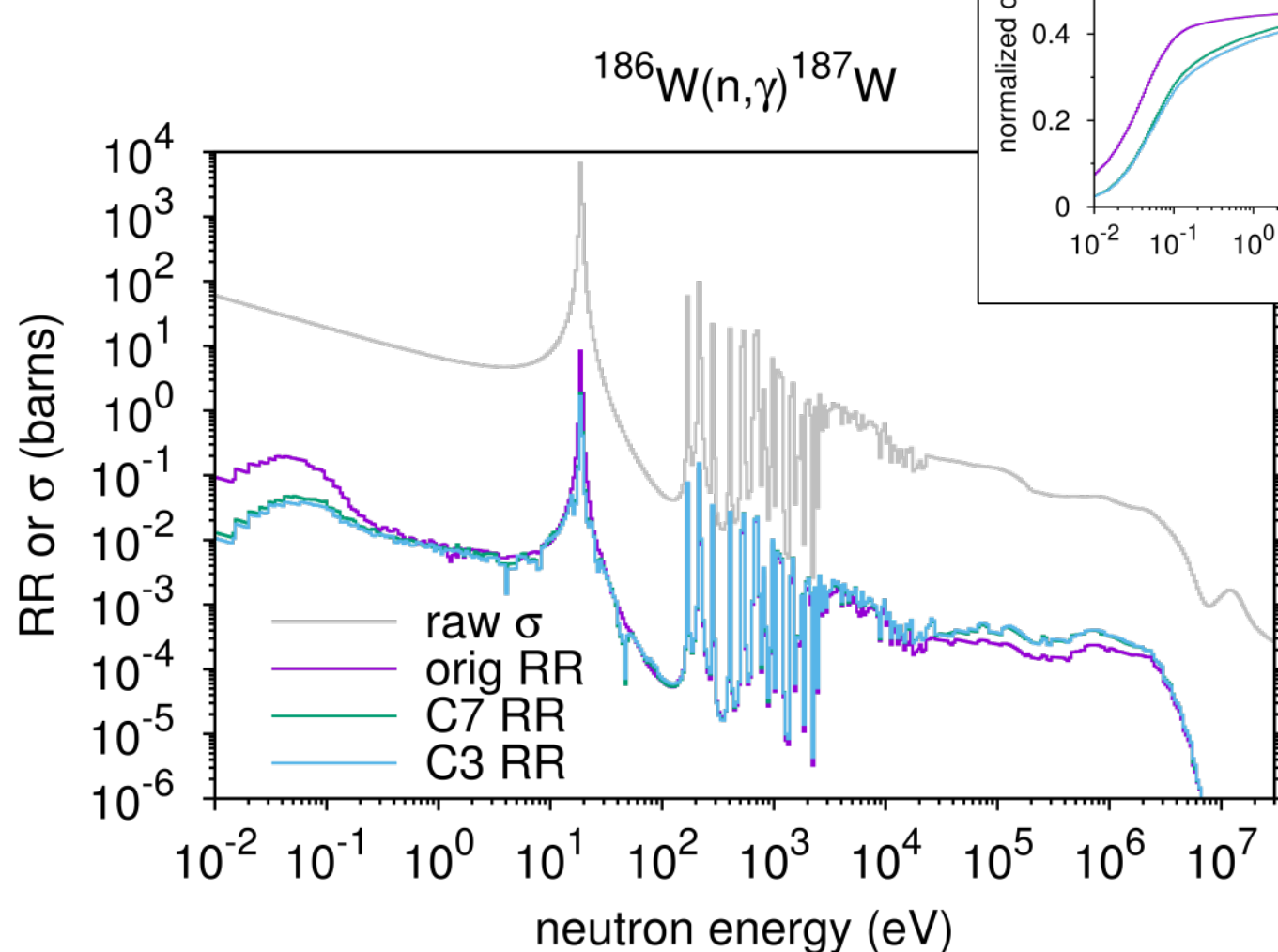
- Main Re isotopes produced during irradiation are  $^{185}\text{Re}$  and  $^{187}\text{Re}$ 
  - Produced via (n, $\gamma$ ) reactions on  $^{184}\text{W}$  and  $^{186}\text{W}$ , followed by  $\beta$ -decay of  $^{185}\text{W}$  ( $T_{1/2}=75$  days) and  $^{187}\text{W}$  (24 hours), respectively.
- Raw total collapsed reaction rate (RR) for these (n, $\gamma$ ) reactions and self-shielding (SS) corrected values:

Reaction	Original spectrum		C7		C3	
	Raw RR	SS RR	Raw RR	SS RR	Raw RR	SS RR
$^{186}\text{W}(\text{n},\gamma)^{187}\text{W}$	22.5 (0.01)	17.2	6.21 (0.09) (-72%)	4.67	5.54 (0.1) (-75%)	4.13
$^{184}\text{W}(\text{n},\gamma)^{185}\text{W}$	0.92 (0.71)	0.60	0.63 (1.8) (-32%)	0.29	0.64 (1.8) (-30%)	0.29

(all RR in barns, black bracket values are +/- errors, green bracket values are % reduction in RR relative to original spectrum)

# Collapsed reaction rates

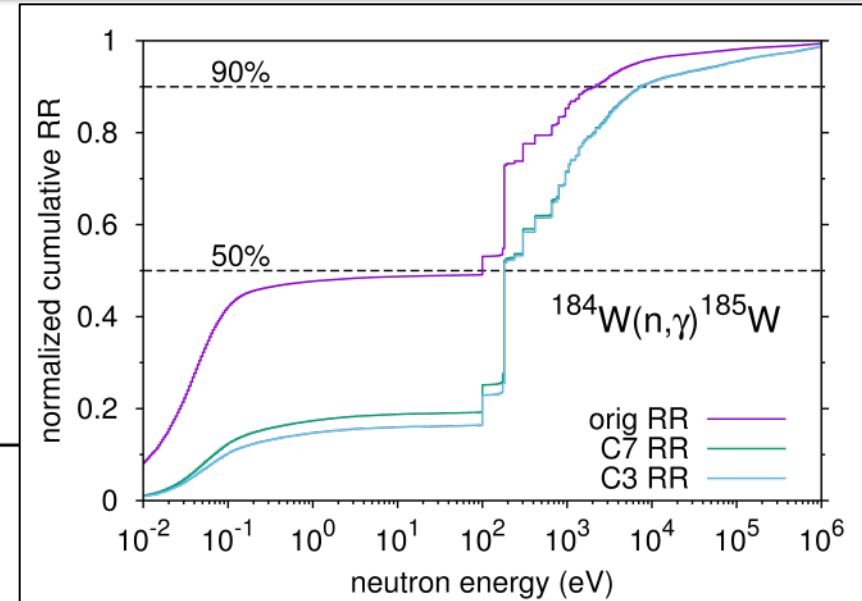
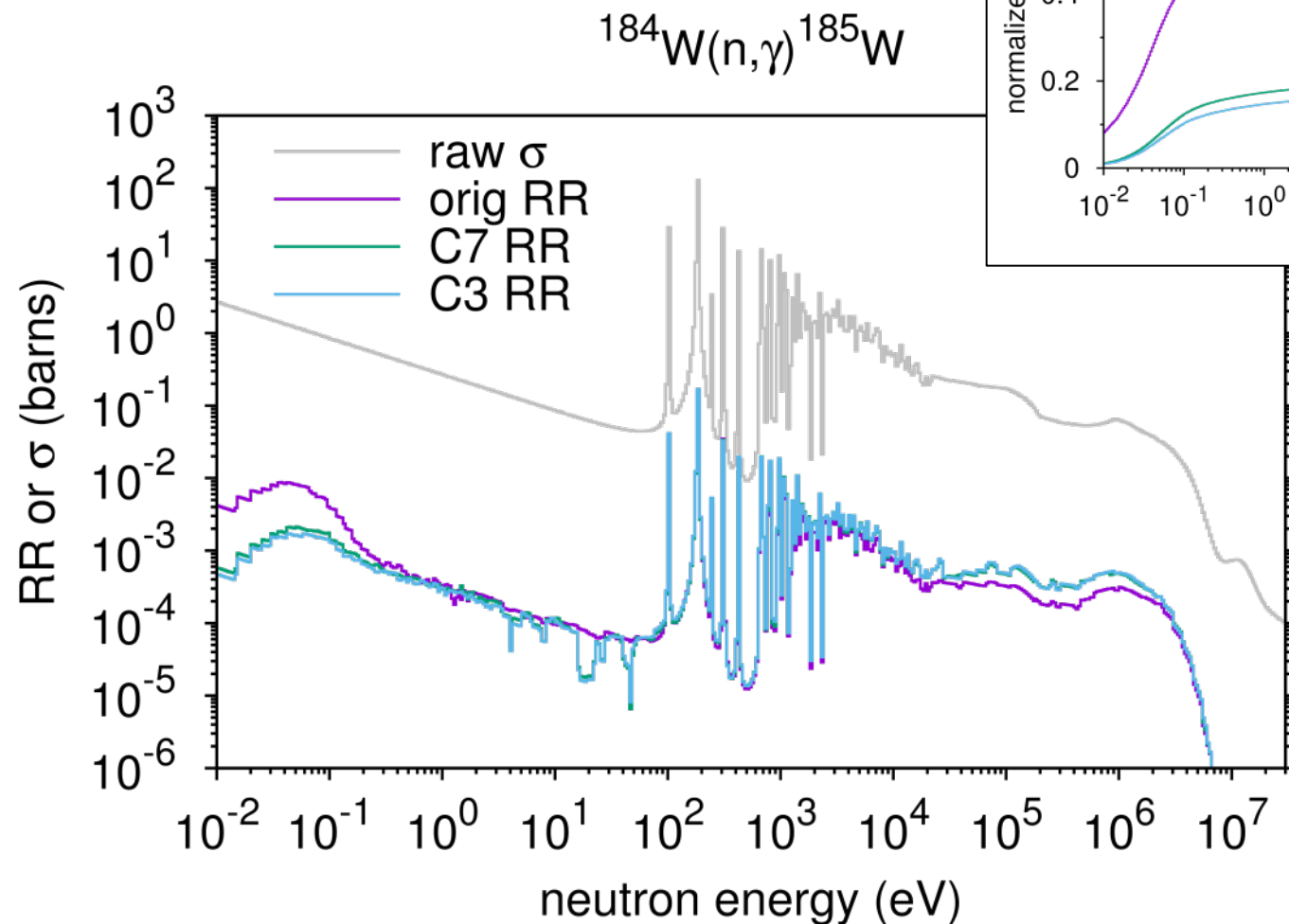
- Almost 50% of RR comes from thermal neutrons below 10 eV




**(RR and  $\sigma$  in a fine group structure with 660 bins below 30 MeV)**

# Collapsed reaction rates

- For new spectra, only 20% of RR comes from thermal neutrons below 100 eV



**(RR and  $\sigma$  in a fine group structure with 660 bins below 30 MeV)**

- Inventory simulation with FISPACT-II of pure tungsten with fully detailed irradiation schedule (including gaps and change in position) and new spectra
  - TENDL 2014 nuclear libraries in 660 energy groups
  - Self-shielding correction of reaction cross sections included (  2% Re predicted without correction)
- Results after 208.26 effective full power days:
  - 1.4 atomic % Re (and 0.1% Os)
    - good agreement with 1.2-1.4% values from measurements
    - And much better than ~4% prediction based on usual HFR neutron spectrum
  - 1.6 effective dpa in the tungsten (using  $E_d = 55$  eV)

- A proper characterization of the neutron spectra for irradiated samples is vital to get even close to real transmutation rate in simulations
  - Without this correct treatment of the neutron fields the reaction rates (and hence transmutation rates) for key capture reactions are much greater
  - The thermal part of the neutron spectrum is very important and must be correctly predicted
- Simulations in W with more realistic neutron spectra give Re production rates that are in very good agreement with experimental measurements
- Further explorations:
  - Properly corrected neutron spectra for W at the sample positions may cause further refinement of results
  - Variation (of Re %) with depth due to self-shielding



- Collaboration with PSI, using modern CASMO-SIMULATE to compare inventory predictions for variety of assemblies:
  - BWR and PWR with mix of UO<sub>2</sub>, MOX, Gd
  - Includes Takahama, Atrium-10, TMI-1, Beznau

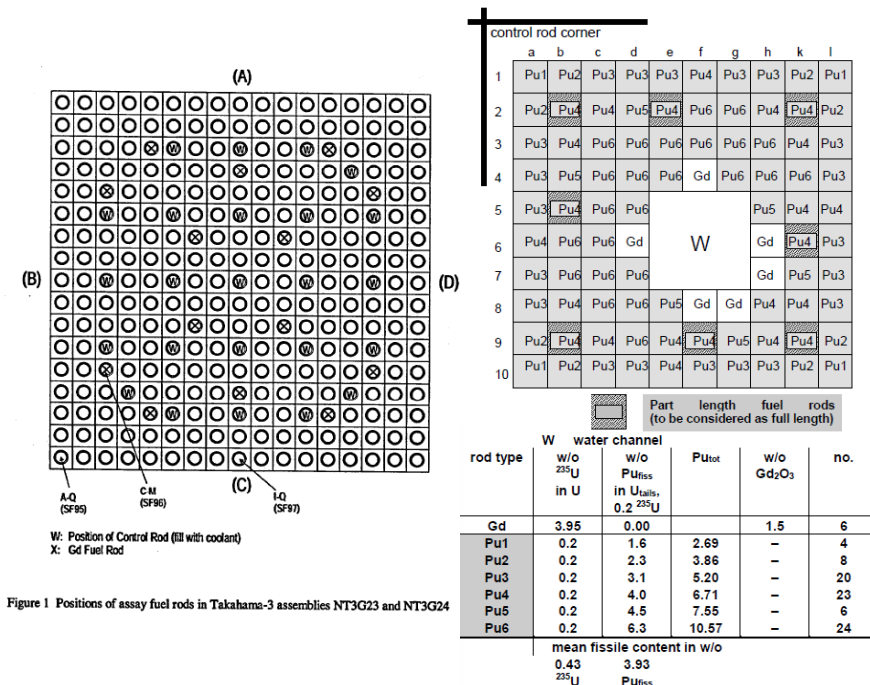
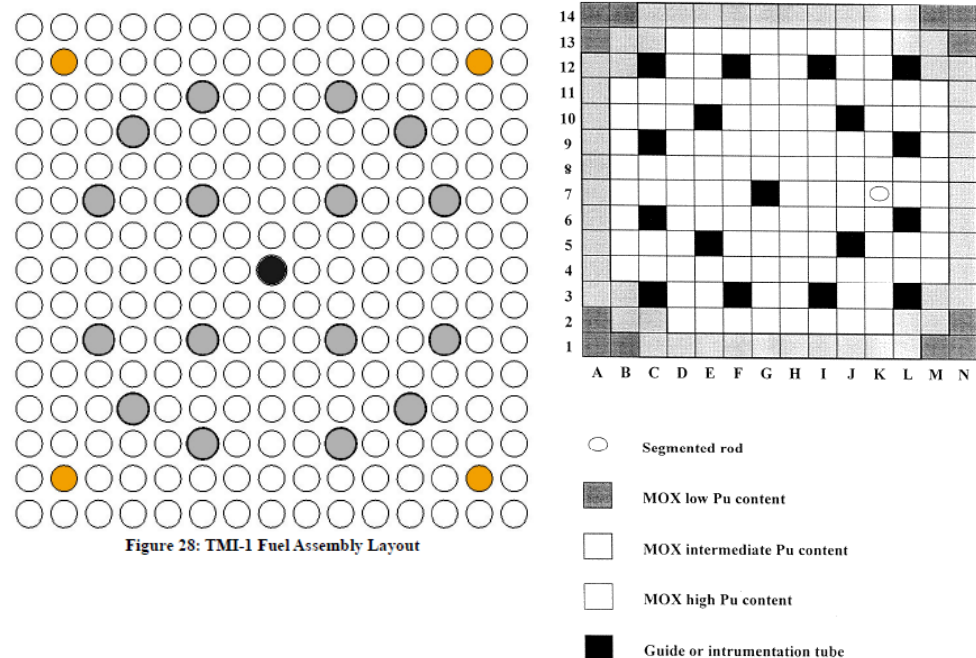
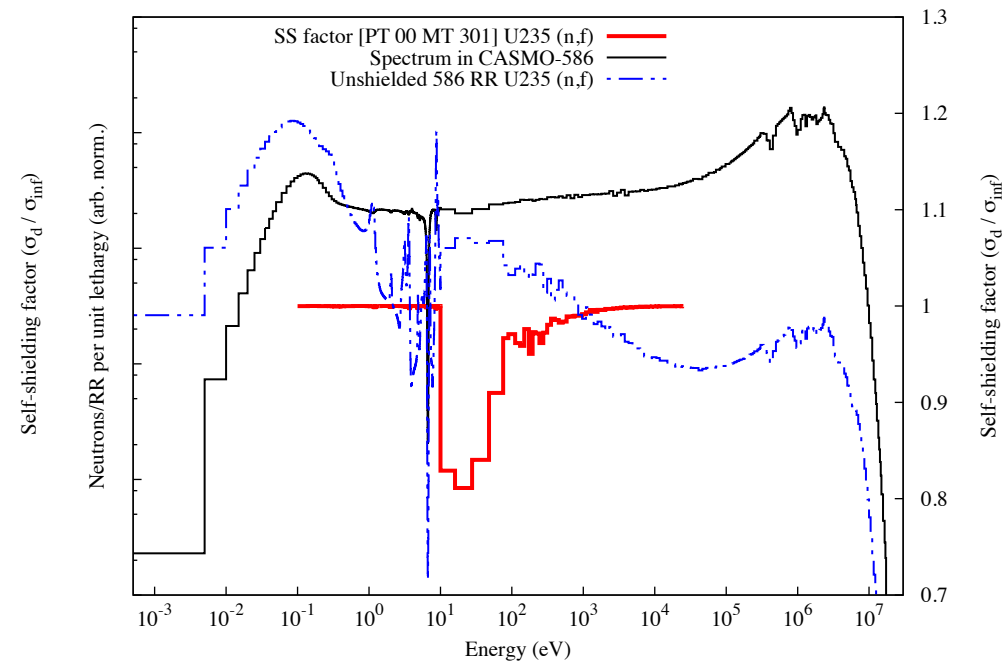
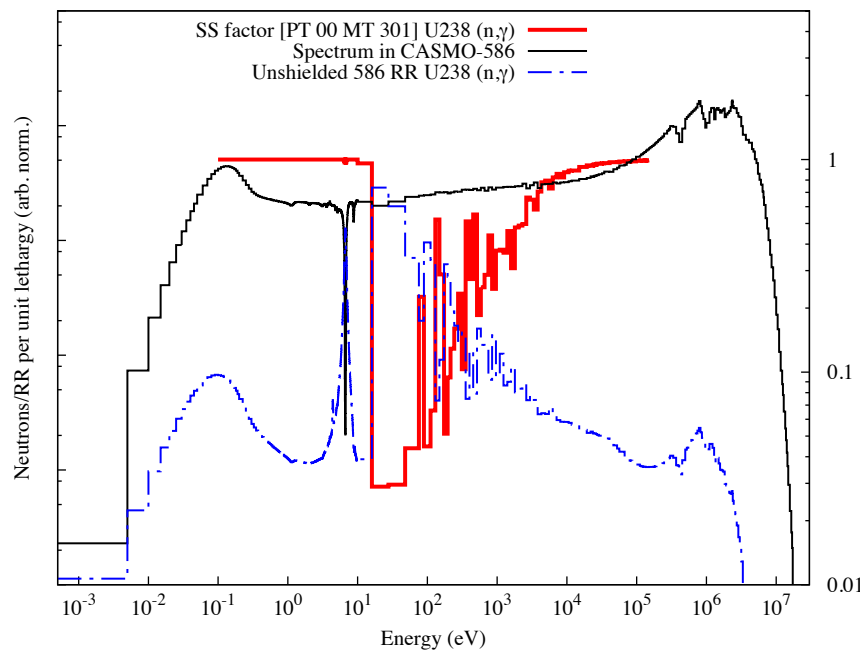


Figure 1 Positions of assay fuel rods in Takahama-3 assemblies NT3G23 and NT3G24



- Added 586 CASMO data for ENDF/B-VII.1, with CALENDF PTs for self-shielding. Applied to major actinides, but can in principle apply to any nuclide
- Left:** U8 capture RR and SSFs **Right:** U5 fission RR+SSFs

Note: CASMO 586 treatment of  $<10$  eV requires no SSFs! No so for  $>10$  eV, where significant SS occurs and must be accounted for.



- In all examples, normalisation using POWER keyword of FISPACT-II (normalising flux based on full Kerma) to CASMO power density, converted to W/cc.
- Ratios are to CASMO simulation, following the spectra changes over 40 GWd/te, **below**: BWR MOX simulation

